International Journal of Nanomedicine

Dovepress
Taylor & Francis Group

Open Access Full Text Article

ORIGINAL RESEARCH

Comparative in vitro Study on Immunomodulatory Effects of Nano-Hydroxpatite Powders on Human Immune Cells

Kamil Grubczak[1], Anna Kretowska-Grunwald[1], Urszula Szalaj[2], Aleksandra Starosz[1], Wojciech Swieszkowski[3], Marcin Moniuszko[1,4]

[1]Department of Regenerative Medicine and Immune Regulation, Medical University of Bialystok, Bialystok, Poland; [2]Laboratory of Nanostructures, Institute of High Pressure Physics, Polish Academy of Sciences, Warsaw, Poland; [3]Faculty of Materials Engineering, Warsaw University of Technology, Warsaw, Poland; [4]Department of Allergology and Internal Medicine, Medical University of Bialystok, Bialystok, Poland

Correspondence: Kamil Grubczak, Department of Regenerative Medicine and Immune Regulation, Medical University of Bialystok, Jerzego Waszyngtona 13, Bialystok, 15-269, Poland, Tel +48 748 59 72, Email kamil.grubczak@umb.edu.pl

Introduction: Significant advancement was recently achieved in the field of hydroxyapatite nanoparticles, contributing to their implementation in numerous biomedical applications, including bone tissue reconstruction. Nevertheless, the influence of these materials on the immune system still remains an unresolved issue.

Materials: Here, we managed to reveal a direct in vitro impact of nano-hydroxyapatite particles on immunological, cellular and humoral components. Further, we analyzed the effect of nanoparticle size and shape on healthy human immune cells residing in the peripheral blood. Special attention was given to particles produced using the microwave hydrothermal synthesis method and precisely controlled size. Viability, phenotypes, activation status, cytokine production and release were assessed using flow cytometry and immunoenzymatic techniques.

Results: We showed that large-sized nanoparticles caused significant induction of immune response associated with innate and acquired immunity, in size-dependent manner. The synthesized nanoparticles allowed for avoidance of the immunogenicity, with no changes in inflammatory cytokines, supporting high biocompatibility. Various effects suggest a different potential use of examined nanoparticles, whether proinflammatory or neutral conditions are required in the field of anticancer therapy or transplantology respectively.

Discussion: Obtained results indicate that precise selection of nano-hydroxyapatites with specific immunomodulatory properties might be crucial for application in the clinical setting. Subsequent studies would establish most suitable therapeutic approaches where selected nano-hydroxyapatites could be implemented.

Plain Language Summary: Nanoparticles are tiny materials with unique properties used in many medical applications, such as bone repair or cancer treatment. One type, called nano-hydroxyapatite (nHAP), is especially promising due to its similarity to human bone. However, we still do not fully understand how these particles affect the immune system, our natural defense network.

In this study, we tested several types of nHAPs to see how they interact with healthy human immune cells. We found that some particles, especially larger ones, can harm immune cells at high concentrations. In contrast, smaller particles had no harmful effects and seemed to be well tolerated.

We also discovered that certain nHAPs changed how immune cells behave. For example, Sigma particles caused monocytes, cells that participate in both inflammatory and non-inflammatory immune response, to shift toward a more inflammatory state. They also increased activity in helper T cells (acquired immunity cells) and led to the production of both protective and inflammatory signaling proteins.

These findings suggest that not all nHAPs are equal. Choosing the right type and size of particle is essential depending on the intended medical use. Some nHAPs may help fight cancer by boosting the immune response, while others could be better suited for treatments requiring low immune activation, such as wound healing or organ transplants. Our research highlights the need for careful design of nanoparticle-based therapies to ensure safety and effectiveness in future clinical applications.

Keywords: nanoparticles, hydroxyapatite, immunomodulation, monocytes, lymphocytes

https://doi.org/10.2147/IJN.S555182
Received: 21 July 2025
Accepted: 19 March 2026
Published: 6 May 2026

Graphical Abstract

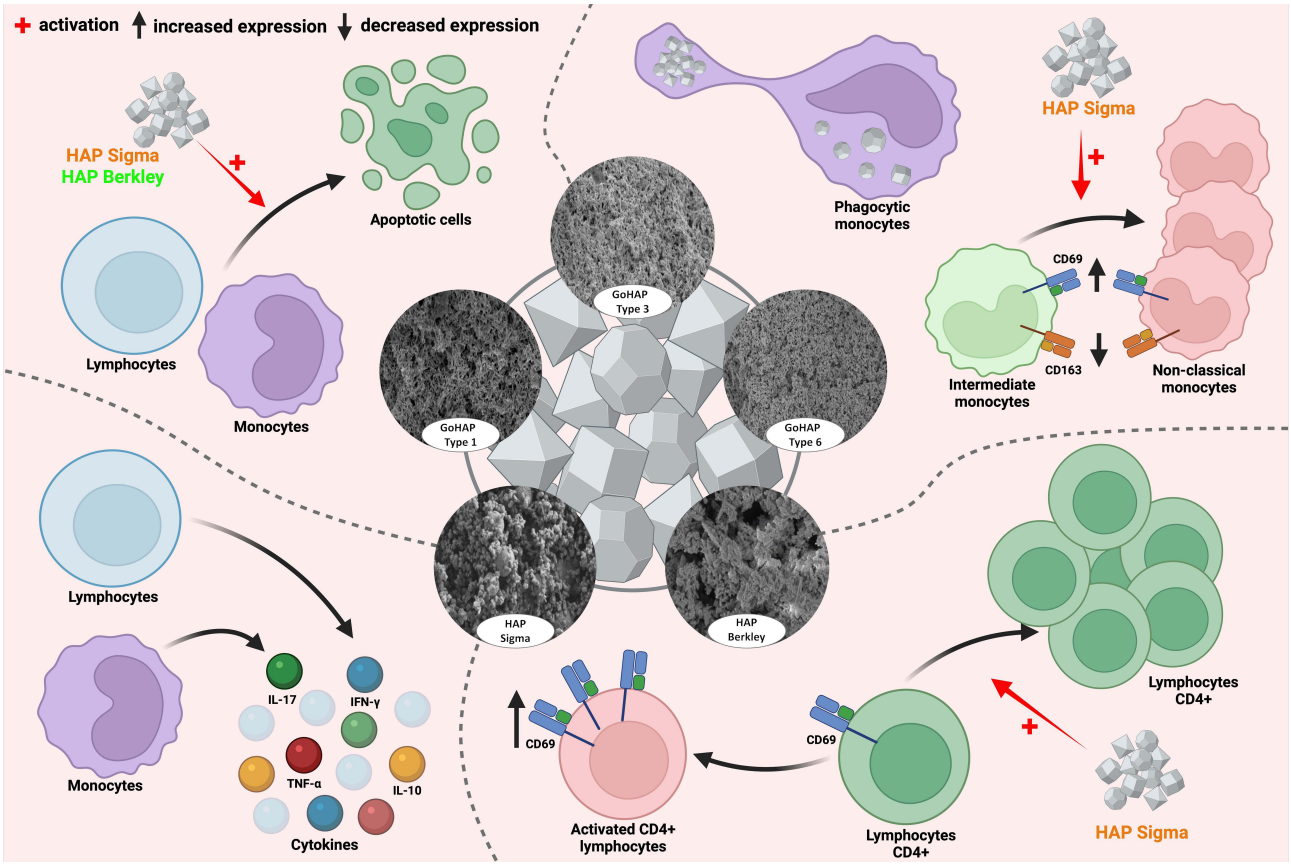

Introduction

Hydroxyapatite (HAP) is a naturally occurring composite of hard tissues of vertebrates.[1] Conventional micro- and macroscale hydroxyapatite have long been used for hard-tissue reconstruction in both orthopedics and dentistry because of their excellent biocompatibility and pronounced osteoconductive behavior, their ability to act as a scaffold for new bone formation. Nanoscale hydroxyapatite preserves these favorable biological properties but, owing to its reduced particle size and markedly increased specific surface area, exhibits additional size-dependent characteristics that have prompted intensive investigation of its potential use in a wide range of biomedical applications, particularly those targeting bone regeneration and other osteogenic processes.[2,3] These crucial features of hydroxyapatite are associated with excellent biocompatibility and the ability of hydroxyapatite-containing scaffolds to support the osteogenic differentiation of stem cells into bone tissue through establishing a favorable osteoimmune microenvironment.[4,5] They possess a unique capability to enter the cell nucleus without any additional agents necessary to disrupt the endosome (cellular uptake) and promote calcium-ion-mediated endosomal escape and cytosolic release of carried particles making them an ideal vector for gene or drug delivery.[6] Additionally, their volumetric stability in granular form makes them a useful component of collagen-rich tissue that is later remodelled into bone, making HAp nanoparticles a desirable substrate in aesthetic medicine and cosmetology.[7] Noteworthy, HAP in the form of a biodegradable nanoparticle - strontium-doped spheres (SHAS) has proven useful in enhancing the efficacy of allergen-specific immunotherapy in mice species.[8] Whereas iron-doped hydroxyapatite nanoparticles (FeHA) were analyzed as a potential agent used in magnetic and nuclear imaging.[9] Moreover, in the study of Badea et al, peppermint essential oil-coated HAP have been found to exhibit higher antimicrobial activity in comparison to uncoated HAP showing their potential role in the reduction of

postoperative implant-related infections. It's important to point out that the addition of the coating did not affect either the size and shape of the tested nanoparticles.[10]

Regardless of their biocompatibility, several studies suggest the possible effect of micrometer-sized hydroxyapatite particles on implant rejection due to their cell toxicity and proinflammatory capabilities.[11] Interestingly, animal experiments with nanoscale hydroxyapatite covered implants showed enhanced infiltration of monocytes/macrophages and lymphocytes (CD4+ predominantly) into the material site.[12] In the in vitro studies of Motskin et al and Huang et al HAP nanoparticles were found to exhibit cytotoxicity towards macrophages, with LDH leakage showing a dose-dependent increase.[13,14] This dependency was similarly observed with regard to lymphocyte viability.[15] However, HAP nanoparticles not only seem to adversely interfere with the proliferation of macrophages but also were found to decrease their phagocytic activity.[16]

The inflammatory response of monocyte subsets seems to depend on HAP crystallinity with amorphous HAP having a more proinflammatory effect than that of crystalline structure, and those synthesized by hard templating stimulating greater secretion of proinflammatory cytokines than those created using soft templating. In line with this, crystalline HAP surfaces, which were found to be more hydrophilic than amorphous HAP, have been associated with a lower proportion of implant-adherent monocytes, consistent with the preferential adhesion of monocytes to hydrophobic, protein-rich interfaces.[17,18] Although HAP nanoparticles are shown to exert an inflammatory response in monocyte subsets, they seem to have a more indirect effect on endothelial cells through an increase in IL-6 production.[19] On the other hand, an analysis of a periprosthetic tissue membrane located between the HAP coating and bone of the removed hydroxyapatite-coated hip prosthesis revealed HAP to be a moderately inert biomaterial as immunohistology only confirmed minor immune cell infiltration.[20] Notably, according to Huang et al HAP nanocrystals do not seem to impact the release of TNF-α from macrophages. These findings contradict their proinflammatory effect presented by Velard et al in their study.[14,18]

Despite the wide range of hydroxyapatite use in the clinical setting, direct effects of their nanoparticle form on the circulating immune system cells remain undiscovered. That corresponds also to the limited data on size and concentration influence of the nanoparticles. Therefore, we found it pivotal to thoroughly assess the impact of hydroxyapatite nanoparticles on the human peripheral blood mononuclear cells (PBMC) considering the broad ongoing research on their application in medicine.

Materials and Methods

Hydroxyapatite Nanoparticles Generation

Five nano-hydroxyapatite materials exhibiting distinct mean particle sizes and morphological characteristics were investigated. Two were commercially available synthetic hydroxyapatite nanopowders obtained from Sigma-Aldrich and Berkeley Advanced Biomaterials. The other three nano-hydroxyapatite materials (GoHAP™ Type1, Type3, and Type6) were synthesized by the co-authors of this study at the Laboratory of Nanostructures, Polish Academy of Sciences using a proprietary, internally developed GoHAP synthesis method.[21] GoHAP hydroxyapatite nanoparticles were obtained with the use of microwave solvothermal synthesis (MSS) method in accordance with the procedures described in the previous publications.[22–24] The following substances were used for GoHAP nanoparticles synthesis: calcium hydroxide ($Ca(OH)_2$, pure); orthophosphoric acid (H_3PO_4, 85% solution, analytically pure); sodium chloride (NaCl, pure) (Chempur, Piekary Slaskie, Poland), deionized water (conductivity <0.1 S / cm, HLP 20UV) (Hydrolab, Straszyn, Poland). Noteworthy, for improved clarity of the investigation, HAP nanoparticles (nHAP) will be referred to throughout the remaining sections primarily by their mean particle size indicating eventually brands to distinguish between slight differences in size: small nHAP (~8–15 nm; GoHAP Type1 and Type3), intermediate nHAP (~40–60 nm; GoHAP Type6 and Berkley-HAP), large nHAP (~90–100 nm; Sigma-HAP).

The MSS method enables the synthesis of hydroxyapatite nanoparticles with precisely controlled mean particle size, including batches that differ from one another by only a few nanometers; therefore, standardized production protocols were established for nanoparticle groups with mean sizes of 8 nm (Type 1), 10 nm (Type 2), 15 nm (Type 3), 23 nm (Type 4), 30 nm (Type 5), and 43 nm (Type 6), and in the present study three of these six GoHAP types - Type 1, Type 3,

and Type 6, were selected for investigation. GoHAP Type1 was obtained by precipitation, with the first step of pouring $Ca(OH)_2$ into 450mL of deionized water followed by addition of 5.7mL of H_3PO_4 into aqueous suspension of $Ca(OH)_2$ using a Titronic Universal digital burette (SI Analytics, Mainz, Germany). Next, reaction mixture was vigorously stirred at room temperature for 30 minutes with SLR magnetic stirrer (SI Analytics, Mainz, Germany). The reaction of GoHAP™ Type1 synthesis was:

$$10Ca(OH)_2 + 6H_3PO_4 \rightarrow Ca_{10}(PO_4)_6(OH)_2(\downarrow) + 18H_2O.$$

Generation of GoHAP Type3 and Type6 was performed by hydrothermal heating of the GoHAP Type1 aqueous suspension with the use of MSS-2 microwave reactor: GoHAP Type3 – 3kW, 90 seconds, 3 bar pressure, equilibrium temperature of 140°C; GoHAP Type6 – 20kW, 1200 seconds, 20 bar pressure, balance temperature of 220°C. Obtained GoHAP hydroxyapatite nanoparticles were shock-frozen with liquid nitrogen and dried in Lyovac GT-2 freeze dryer (SRK Systemtechnik GmbH, Riedstadt, Germany).

Characterization of Hydroxyapatite Nanoparticles

Nano-hydroxyapatite particles characterization was performed in accordance with ISO 17025:2005 at accredited testing laboratory no. AB 1503. Specific Surface Area (SSA) of GoHAP nanoparticles was determined by BET adsorption method (Brunauer-Emmett-Teller) using Gemini 2360 surface analyzer (Micrometrics, Norcross, USA) according to ISO 9277:2018–02. Skeletal density of the samples was measured using AccuPyc II 1340 helium pycnometer (Micrometrics, Norcross, USA) in accordance with ISO 12154:2014. Prior to measurement of the mentioned parameters, nanoparticles were desorbed in a VacPrep 061 desorption station (Micrometrics, Norcross, USA) at the temperature of 150°C, for 1.5 hours, under vacuum. Next, Sauter mean diameter of hydroxyapatite nanoparticles was calculated on the basis of (aspherical shape was assumed):

$$Sauther\ Mean\ Diameter = \frac{A}{SSA \cdot 10^{18} \cdot 10^{-21}}\,[nm]$$

A = shape factor (equal to 6 for the sphere)
SSA = specific surface area [m^2/g]
DEN = skeletal density [g/cm^3]

The calculated Sauter Mean Diameter was subsequently used as the mean particle size. AccuPyc II 1340 FoamPyc V1.06 helium pycnometer was also used for adsorption isotherm determination, at the temperature of 23 ± 1°C, further analyzed with the use of MicroActive software V4.03 (Interactive Data Analysis Software, Micrometrics). Total pore volume of samples was estimated on the basis of adsorbed nitrogen amount at $P/P_0 = 0.9896$. Morphology of nano-hydroxyapatite particles was evaluated using Ultra Plus scanning electron microscope (SEM) (Carl Zeiss Mediatec AG, Jena, Germany), combined with FEI Talos F200X secondary electrons (SE) detector (Thermo Fisher Scientific, Waltham, USA) – beam energy set to 2keV. For SEM observation, a thin layer of platinum-palladium was deposited on the nanoparticles with the sprayer. Diffraction patterns of the X-ray powder diffraction (XRD) were obtained using X'Pert PRO X-ray powder diffractometer (Panalytical Company, Netherlands), equipped with a copper anode (CuKα1) and an ultra-fast PIXcel 1D detector. Analysis was conducted at room temperature, in the 2 theta range from 10° to 100°, with a step of 0.02°. Diffraction patterns were fitted in the Fityk software. Then, assessment of XRD line profiles was performed with the use of analytical formula for polydispersive powders,[25,26] and incorporation of Nanopowder XRD Processor online available demo tool. Furthermore, thermogravimetric analysis (TG+) was performed using STA 449 F1 Jupiter gas-tight thermal analysis system (Netzsch, Selb, Germany). Analysis was carried out with a heating rate of 2°C/min, up to the temperature of 800°C, with measurement performed under constant flow of helium at 60mL/min (Figure 1A–C and Table 1).

Isolation of Peripheral Blood Mononuclear Cells

Leukocyte mass routinely subjected to utilization after processing of blood collected from healthy volunteers admitted at Regional Blood Donation and Treatment Center in Bialystok (Poland) was used for isolation of peripheral blood mononuclear cells (PBMC). Following dilution with phosphate-buffered saline (PBS, Corning) containing 2mM

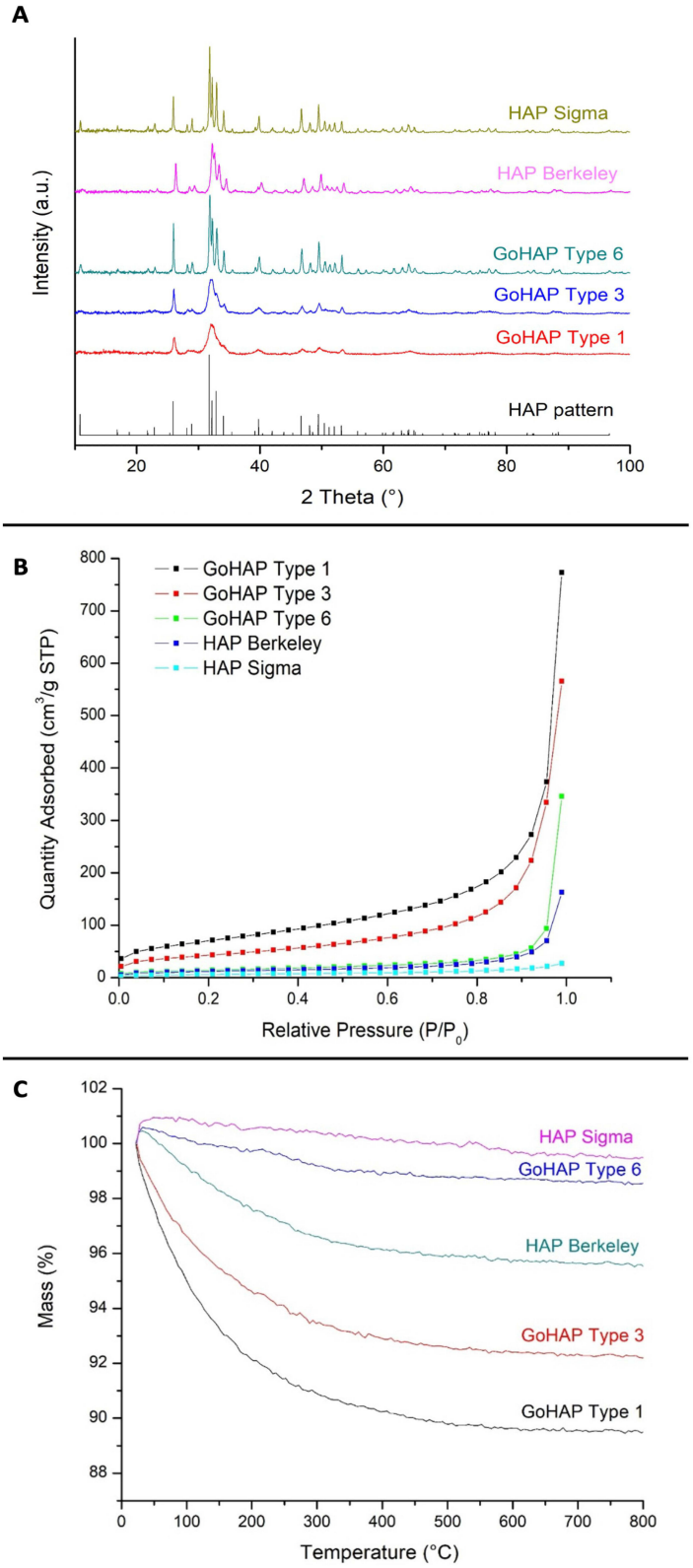

Figure 1 Characteristics of the synthesized nanoparticles. X-ray diffraction lines of selected nano-hydroxyapatites (**A**). Isotherms of the nitrogen absorption on the nanoparticle surface (**B**). Results of thermogravimetric analysis of nano-powders, heated in helium atmosphere from room temperature to 800°C at a rate of 2°C/min (**C**).

https://doi.org/10.2147/IJN.S555182

Table 1 Descriptive Parameters of Tested Nanoparticles

Sample Name	SMD_{BET} (nm)	SSA ± σ (m^2/g)	DEN ± σ (g/cm^3)	TPV (cm^3/g)
GoHAP Type 1	8	251±3	2.85±	1.195
GoHAP Type 3	14	152±3	2.93±	0.874
GoHAP Type 6	40	49±3	3.12±	0.534
HAP Berkeley	51	41±3	2.91±	0.252
HAP Sigma	96	21±3	3.04±	0.042

Abbreviations: SMDBET, BET-based mean particle size; SSA, specific surface area; DEN, skeleton density; TPV, total pore volume.

EDTA (Invitrogen) PBMCs were isolated with the use of gradient density centrifugation technique on Pancoll 1.077 g/mL (PAN Biotech). Following collection of the PBMC fraction, cells were washed several times in PBS with 2mM EDTA and subsequently suspended at the concentration of 1×10^6 cells/mL in complete culture medium: RPMI-1640 (PAN Biotech) with 10% fetal bovine serum (FBS, PAN Biotech) and gentamicin (Gibco). Prior to the biological material collection, the informed consent was obtained from all the subjects enrolled in the study. The local Bioethical Committee in Bialystok approved the implemented study protocol, approval number: APK.002.272.2020.

Cell Culture of PBMC with Hydroxyapatite Nanoparticles

Prepared PBMCs were distributed on 24-well cell culture plates at the concentration of 1×10^6 cells/mL in complete culture medium. Next, selected hydroxyapatite nanoparticles, including small nHAP (~8–15 nm; GoHAP Type1 and GoHAP Type3), intermediate nHAP (~40–50 nm; GoHAP Type6 and Berkley-HAP), large nHAP (~90–100 nm; Sigma-HAP), were applied on PBMC to obtain several different concentrations: 20μg/mL, 100μg/mL, 500μg/mL and 1000μg/mL. Peripheral blood cells were incubated in the presence of nanoparticles for 24 hours in 37°C, 5% CO_2. Following incubation cells were centrifuged to obtain supernatants (collected and frozen at −80°C) and PBMC pellet used directly for flow cytometric assessment.

Colorimetric Evaluation of Cellular Cytotoxicity in PBMC Treated with Nanoparticles

LDH activity was measured in the collected supernatants for the assessment of cellular cytotoxicity in PBMC subjected to hydroxyapatite nanoparticles presence. Tested samples were applied on 96-well plates and LDH Cytotoxicity Assay Kit (Pierce) was used to measure the conversion of tetrazolium salt (INT) to red formazan product associated with LDH activity. Intensity of colorimetric reaction was measured at 490nm wavelength using LEDETECT 96 Microplate Reader (Labexim Products Co., Lengau, Austria).

Flow Cytometric Analysis of PBMC Viability, Activation Status and Cytokine Production

Viability assessment within lymphocytes and monocytes, was performed with the use of 7-aminoactinomycin D (7AAD) and APC-conjugated Annexin V. Following 15-minute staining, at room temperature, in the dark, the cells were immediately analyzed on the flow cytometer. Gating of lymphocytes and monocytes was based on morphological properties - forward scatter (FSC; relative size) and side scatter (SSC; relative granularity), and fluorescence related to 7AAD and Annexin V. Accordingly, three cell populations have been distinguished within the studied populations of

immune cells: viable (7AAD- AnnexinV-), early apoptotic (7AAD-AnnexinV+), late apoptotic (7AAD+ AnnexinV+) (Supplementary Figure 1A).

Assessment of monocyte and lymphocyte subsets frequencies, and their activation status required use of fluorochrome-conjugated monoclonal antibodies, including anti-CD4 FITC (RPA-T4), anti-CD8 PE (HIT8α), anti-CD14 PerCP (MϕP9), anti-CD16 FITC (3G8), anti-CD69 APC (H1.2F3), anti-CD25PE-Cy5 (M-A251), and anti-CD163 PE (GHI/61) (BD Bioscience). Staining for 25 minutes, at room temperature, in the dark, was followed by washing out unbind antibodies in PBS and fixing cells using Cell Fix reagent (BD Bioscience). Flow cytometric analysis was based on gating involving FSC/SSC properties, and differential CD4/CD8 expression to distinguish CD4+ (helper T cells) and CD8+ (cytotoxic T cells) lymphocytes (Supplementary Figure 1B) or CD14/CD16 expression to gate CD14++CD16- (classical), CD14++CD16+ (intermediate), CD14+CD16++ (non-classical) monocytes (Supplementary Figure 1C). Within CD4+, CD8+ and total lymphocytes, the frequency of positive cells and mean expression (mean fluorescence intensity, MFI) of early (CD69) and late (CD25) activation markers was evaluated (Supplementary Figure 1B). Regarding total monocytes and monocyte subsets, changes in CD69 (activation marker) and CD163 (differentiation marker) were measured to establish the activation/differentiation status (Supplementary Figure 2A). In addition, MFI of FSC and SSC parameters were analyzed for evaluation of size and internal structure (granularity) of monocytes resulting from nanoparticles engulfment (Supplementary Figure 1C).

Analysis of intracellular production of selected cytokines in monocytes and lymphocytes was performed following extracellular staining with anti-CD4 FITC for lymphocytes, and anti-CD14 PerCP and anti-CD16 FITC for monocytes, and additional permeabilization step using FACS Permeabilization Solution 2 (BD Bioscience). Next, intracellular staining was performed with the use of anti-TNF-alpha PE (clone Mab11) and anti-IL-10 PE (clone JES3-9D7) in monocytes, and anti-IFN-gamma PE-Cy7 (clone B27), anti-IL-10 PE, anti-IL-17A Alexa647 (clone SCPL1362) in lymphocytes. CD4+ lymphocytes and subsets of monocytes were distinguished as described in the previous paragraph, then frequency of cells producing certain cytokines or mean expression of them was measured in gated subpopulations (Supplementary Figure 2B). Flow cytometric data were acquired using FACS Calibur flow cytometer (BD Bioscience, San Jose, USA) and subsequently analyzed in FlowJo software (Tree Star Inc., Ashland, USA).

Immunoenzymatic Assessment of Selected Cytokines Released by PBMC

Supernatants collected after PBMC culture in the presence of nanoparticles were subjected to enzyme-linked immunosorbent assay (ELISA) for evaluation of IFN-gamma, TNF-alpha and IL-10 production by cells. DuoSet kits (R&D Systems) were used, thus first, 96-well plates were coated with capture antibody (anti-TNF-alpha, anti-IFN-gamma or anti-IL-10) followed by intensive washing steps and blocking reagent diluent (1% BSA in PBS). Next, the tested supernatants and standards were applied, incubated for 2 hours at room temperature and washed out. The following 2-hour incubation was preceded by adding biotinylated detection antibody (mouse in IFN-gamma, goat in TNF-alpha and IL-10 kit). The last two 20-minute incubations were associated with streptavidin-HRP B and substrate solution (TMB Reagent Kit, BD Bioscience) which were added subsequently. Finally, the reaction was stopped by 2N H_2SO_4 (Sigma-Aldrich) and optical density was determined immediately at 450nm wavelength with the use of LEDETECT 96 Microplate Reader (Labexim Products Co., Lengau, Austria).

Results

Evaluation of Generated Hydroxyapatite Nanoparticles Characteristics

The physicochemical properties and morphology of the nanomaterials used in this study are summarized in Figure 1. XRD analysis confirmed that each of the five investigated nanomaterials corresponded to phase-pure hydroxyapatite (Figure 1A). The determined adsorption isotherms (Figure 1B) and thermogravimetric analysis (Figure 1C) showed trends consistent with the SSA and SMD_{BET} values obtained for the individual nanomaterials. The specific surface area and the corresponding mean particle size differed markedly among the tested nanopowders. As expected, small nHAP (~8–15 nm; GoHAP Type1) exhibited the highest SSA, whereas the lowest SSA was observed for large nHAP (~90–100 nm; Sigma HAP). Small nHAP - GoHAP Type1, demonstrated the mean particle size of 8nm with a needle-like shape.

 https://doi.org/10.2147/IJN.S555182

Another small size nHAP - GoHAP Type3, with mean particle size of 14nm, present as more elongated particles compared to Type1. Intermediate nHAP - GoHAP Type6, present oval shaped with mean particle size of 40nm. Overall, the GoHAP nanoparticles (small to intermediate nHAP) exhibited broadly comparable morphology across the series; however, they were classified into types according to the MSS synthesis method, where an increasing type number corresponds to a larger mean particle size. With increasing particle size, the morphology progressively shifts from predominantly needle-like to more spherical particles (Figure 2A–C). The purchased Berkeley HAP nanoparticles (intermediate nHAP) were supplied as granules composed of loosely packed hydroxyapatite nanoparticles, for which the calculated mean particle size of the primary particles was 51 nm. The diameter of the nanoparticle-assembled granules ranged from 5 to 51 μm and was determined from SEM micrographs using ImageJ software (Figure 2D). In contrast, Sigma-HAP (large nHAP) exhibited a substantially larger calculated mean particle size of 96 nm; in addition to individual nanoparticles, spherical micrometric structures with sizes of 0.2–0.8 μm were also observed. Distinct grain boundaries indicate that these granules correspond to sintered Sigma HAP particles (Figure 2E).

Assessment of Peripheral Blood Mononuclear Cells Viability in the Presence of Hydroxyapatite Nanoparticles

Initially, the evaluation of PBMC viability in the presence of hydroxyapatite nanoparticles was performed using the measurement of LDH activity (indicator of cellular cytotoxicity) in the supernatants after 24 hours of incubation. We found that none of GoHAP group nanoparticles (small to intermediate nHAP) caused significant changes in total PBMC LDH activity indicating no effect on the viability of peripheral blood immune cells. On the contrary, large nHAP (~90–100 nm; Sigma-HAP) demonstrated increased cytotoxicity through higher levels of LDH activity at concentrations of 1000μg/mL. A slight tendency for higher LDH activity levels was also observed in reference to another intermediate nHAP (~40–60 nm; Berkley-HAP), but only at 20μg/mL (Figure 3A).

Peripheral blood lymphocytes' viability was predominantly affected by intermediate to large nHAP (~96 nm, Sigma-HAP; ~51 nm, Berkley-HAP). Slight changes were associated with a decline in viability of those cells with concomitant increase in early apoptotic cells frequency. The small nHAP from GoHAP group did not cause adverse effects on lymphocyte viability in the studied samples (Figure 3B). Regarding monocytes, the presence of small nHAP (GoHAP Type1) and intermediate nHAP (GoHAP Type6) led to a slight elevation of viable cells at 1000μg/mL (starting at 100μg/mL for GoHAP Type1). Similar changes were observed in the presence of another intermediate nHAP (Berkley-HAP), however, its activity between the concentration of 20 to 100μg/mL was additionally associated with higher early apoptotic cell levels. Furthermore, large nHAP (~90–100 nm; Sigma-HAP) caused a significant dose-dependent increase in late apoptotic cells (Figure 3C). Noteworthy, the best stability of the viability parameters, within lymphocytes and monocytes, was observed in the presence of small nHAP (~14 nm; GoHAP Type3) (Figure 3B and C).

Evaluation of Phagocytosis Related Changes in the Size and Granularity of Monocytes in the Presence of Hydroxyapatite Nanoparticles

Increased granularity (SSC parameter) of monocytes following incubation with nano-hydroxyapatites indicates enhanced phagocytosis of those elements. The highest rate of these changes was observed in reference to large nHAP (~90-100 nm; Sigma-HAP), in dose-dependent manner. Importantly, the granularity of monocytes was significantly higher in the presence of large nHAP compared to other studied nanoparticles. Similar direction of changes was also observed in reference to intermediate nHAP (GoHAP Type6), predominantly at concentrations of 500μg/mL and higher. Despite elevated levels of SSC also in the remaining types of nanoparticles, the changes in the internal structure of monocytes were less pronounced (Figure 4A).

Apart from large nHAP (Sigma-HAP), the size of monocytes remained relatively stable (FSC parameter) in the presence of other tested nanoparticles. Noteworthy, we observed a significant increase in the size of CD16-positive monocyte subpopulations subjected to incubation with these nanoparticles. Those elevated levels of the FSC parameter shown statistical significance only at the highest tested concentration of 1000μg/mL Figure 4B).

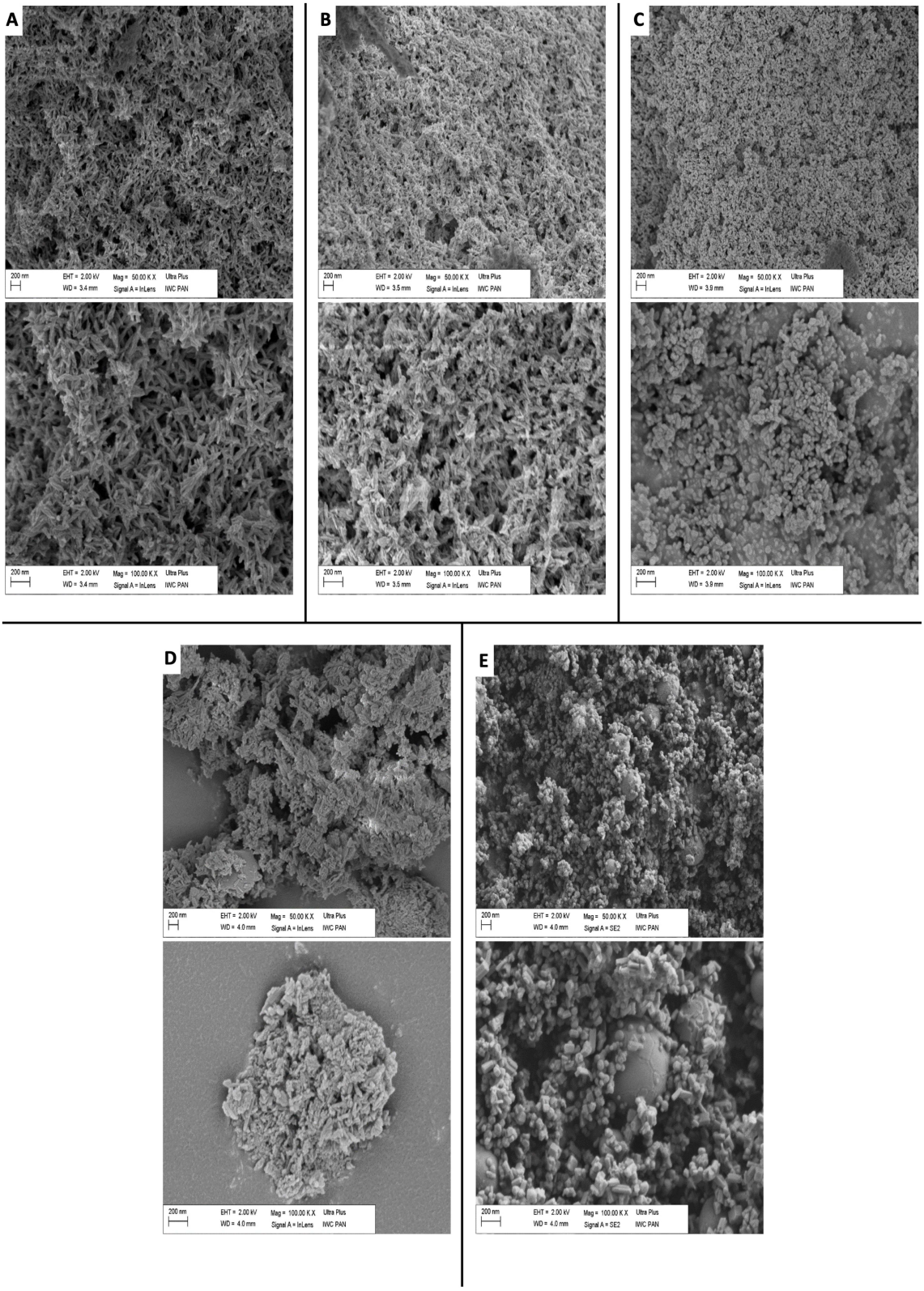

Figure 2 Scanning electron microscopy (SEM) pictures of tested hydroxyapatite nanoparticles. Visualization was performed at 50,000 and 100,000x magnification for each analyzed nano-hydroxyapatite type: GoHAP^{TM} Type 1 (**A**), GoHAP^{TM} Type 3 (**B**), GoHAP^{TM} Type 6 (**C**), HAP Berkley (**D**), HAP Sigma (**E**).

https://doi.org/10.2147/IJN.S555182

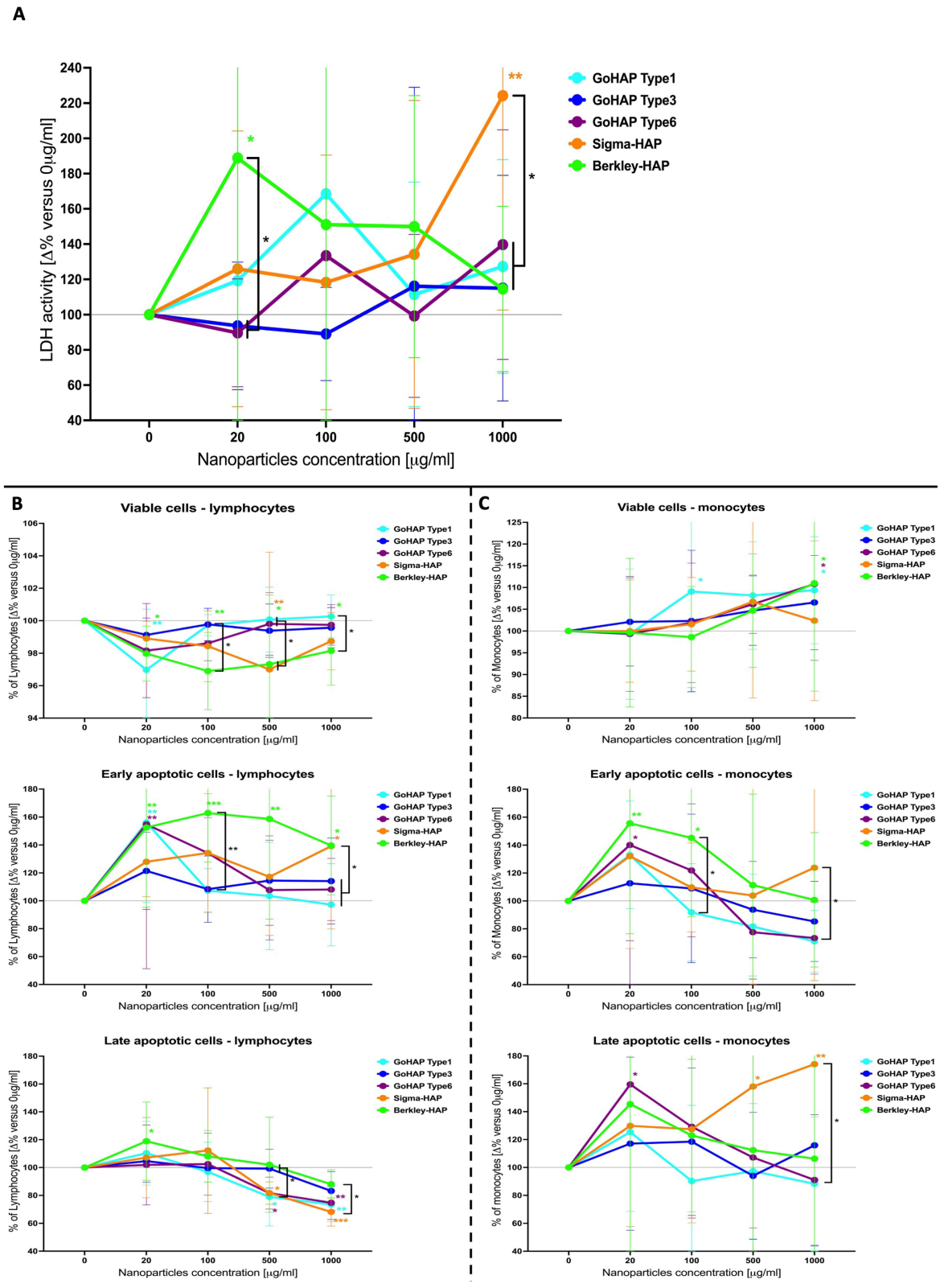

Figure 3 Evaluation of selected nanoparticles effect on viability of immune cells. LDH activity measurement in supernatants of PBMC incubated with nano-powders (**A**). Flow cytometric assessment of viability parameters was performed individually within peripheral blood lymphocytes (**B**) and monocytes (**C**). Data presented as median change (with interquartile range) versus untreated samples (0μg/mL) (n = 8). Statistically significant differences versus untreated samples indicated with color asterisks linked to selected nanoparticles; brackets indicate differences between types of nano-powders at certain concentrations, as determined by two-way ANOVA followed by Fisher's LSD post hoc test. Significance level was set at p value of 0.05: *< 0.05, **< 0.01, ***< 0.001.

https://doi.org/10.2147/IJN.S555182

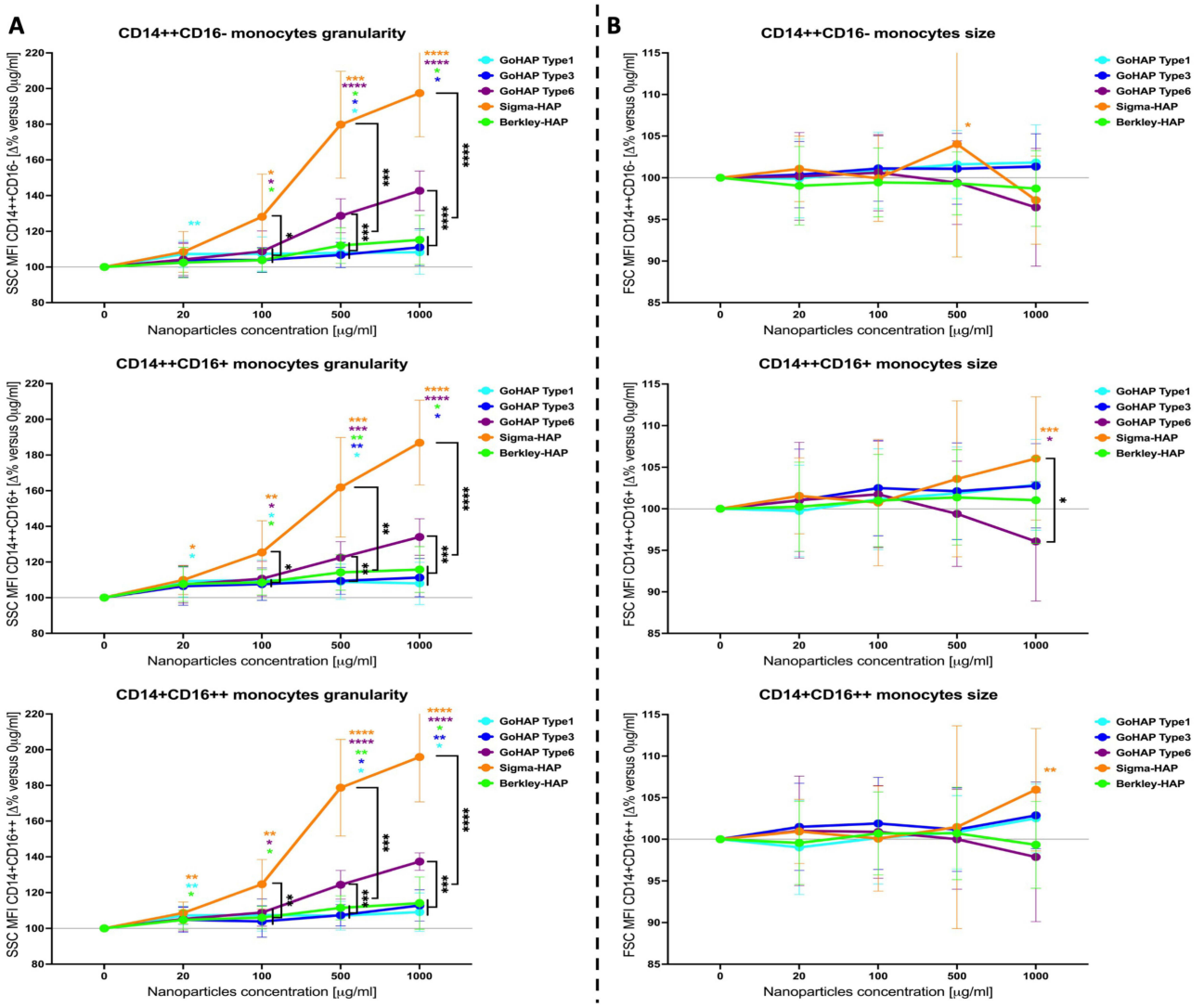

Figure 4 Assessment of selected nanoparticles effect on size and granularity of monocyte subsets. Analysis of relative size (**A**) and granularity (**B**) changes in monocyte subsets incubated in presence of nano-hydroxyapatites. Data presented as median change (with interquartile range) versus untreated samples (0μg/mL) (n = 8). Significant differences versus untreated samples were indicated with color asterisks corresponding to selected nanoparticles; brackets demonstrated differences between types of nano-powders at certain concentrations, as determined by two-way ANOVA followed by Fisher's LSD post hoc test. Significance level was set at p value of 0.05: *< 0.05, **< 0.01, ***< 0.001, ****p < 0.0001.

Evaluation of Hydroxyapatite Nanoparticles Influence on Monocyte Subsets Frequency and the Cells Activation Status

Presence of large nHAP (~90-100 nm; Sigma-HAP) was associated with an increased frequency of classical CD14++CD16- monocytes, reported at concentrations starting at 500μg/mL. Higher rate of changes was reported in non-classical CD14+CD16++ monocytes, with a clear dose-dependent manner. Interestingly, intermediate CD14++CD16+ monocytes showed depletion in percentage when incubated with large nHAP. No substantial differences were found in reference to the remaining types of nano-hydroxyapatites. However, to a slight extent, intermediate nHAP (GoHAP Type6) seems to influence classical and intermediate subpopulations in the same way as large nHAP (Sigma-HAP). Noteworthy, large nanoparticles caused significant changes in monocyte subsets additionally when compared to other tested nanoparticles at selected concentrations (Figure 5A).

Large nHAP (Sigma-HAP) were furthermore the dominant elements affecting the activation status of monocyte subsets. These nanoparticles led to a significantly higher frequency of activated, CD69-positive, intermediate and non-classical monocyte subsets. Changes occurred at the concentration of 500μg/mL and higher, and were the most visible in

https://doi.org/10.2147/IJN.S555182

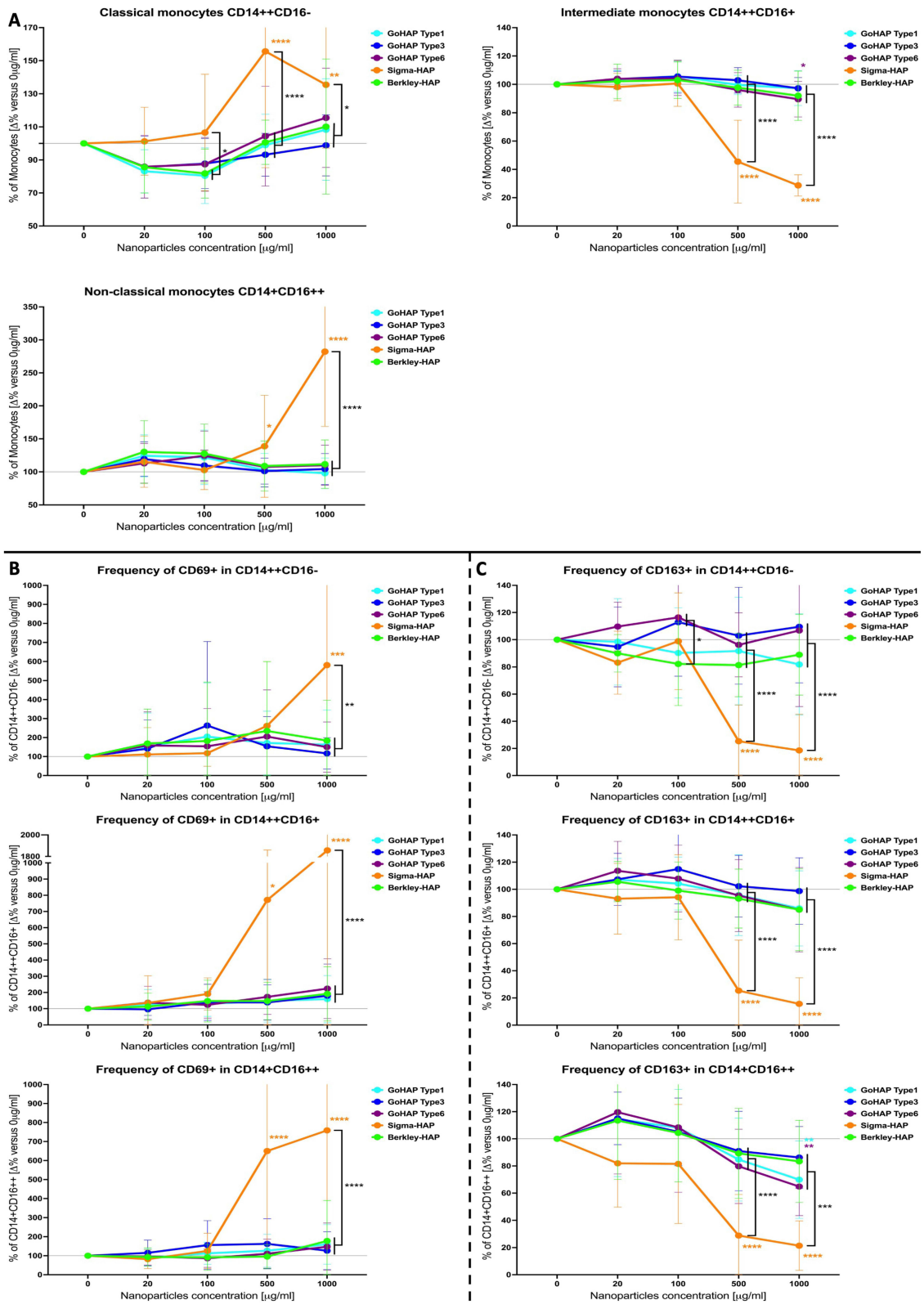

Figure 5 Analysis of frequencies and activation status of monocyte subpopulations stimulated with nano-hydroxyapatites. Changes in monocyte subsets frequency in presence of nanoparticles (**A**). Assessment of activation markers – CD69 (**B**) and CD163 (**C**), in monocyte subsets incubated with nanoparticles. Data presented as median change (with interquartile range) versus untreated samples (0μg/mL) (n = 8). Significant differences versus untreated samples indicated with color asterisks corresponding to selected nanoparticles; brackets demonstrated differences between types of nano-powders at certain concentrations, as determined by two-way ANOVA followed by Fisher's LSD post hoc test. Significance level was set at p value of 0.05: *< 0.05, **< 0.01, ***< 0.001, ****p < 0.0001.

https://doi.org/10.2147/IJN.S555182

CD14++CD16+ monocytes. Importantly, elevated levels of activated classical CD14++CD16- monocytes were only reported at the 1000μg/mL of large nanoparticles. With only minimal variations at the tested concentrations, no significant changes in CD69-related activation of monocytes were found when incubated with other studied nanoparticles (Figure 5B).

Regarding the differentiation status of monocytes based on the CD163 marker, large nHAP (Sigma-HAP) substantially reduced the frequency of all monocyte subsets with the expression of CD163. Decrease in CD163-positive monocytes was observed within the range of 500μg/mL to 1000μg/mL of nano-hydroxyapatites, and was comparable among different monocyte subpopulations. Among other tested nanoparticles, we showed the reduction of CD163+ non-classical monocytes also when the cells were incubated with small HAP (~8 nm; GoHAP Type1) and intermediate nHAP (~51 nm; GoHAP Type6). Those effects were significantly less strong than those observed in the samples treated with Sigma-HAP (Figure 5C).

Evaluation of Hydroxyapatite Nanoparticles Influence on CD4+ (Helper) and CD8+ (Cytotoxic) Lymphocyte Subpopulations Frequency and the Cells' Activation Status

Contrasting effects were achieved in reference to CD4+ (Th) lymphocytes frequency in samples incubated with nano-hydroxyapatites. Apart from small nHAP (~8 nm; GoHAP Type1), the tested materials led initially to the reduction of CD4-positive T cells at concentration of 20μg/mL. Further increases in the concentration were associated with an increase in that parameter in samples treated with large nHAP (Sigma-HAP), resulting in a significantly higher frequency of CD4+ lymphocytes at 1000μg/mL. The remaining nanoparticles maintained a lower level of Th cells, with the further slight reduction in the presence of small nHAP (~15 nm; GoHAP Type3), and a minimal increase when higher concentrations of intermediate nHAP (~51 nm; GoHAP Type6) were used. In contrast to CD4-related data, none of the selected nano-hydroxyapatites influenced changes in the percentage of CD8-positive (Tc) lymphocytes. Nonetheless, large nHAP (Sigma-HAP) showed significantly lower values compared to small nHAP (GoHAP Type3) at 500μg/mL (Figure 6A).

Lymphocytes affected by the tested nanoparticles seemed to respond in a similar way to monocytes in the context of activation status. In general, large nHAP (Sigma-HAP) presence led to an elevated frequency of early activated CD69+ lymphocytes. That effect was especially seen at the highest concentrations – 500 to 1000μg/mL also when analyzing CD4 + and CD8+ T cells individually. Noteworthy, despite less intensified changes, a gradual increase in reference to CD8-positive lymphocytes was observed starting at even 20μg/mL of these nanoparticles. Interestingly, comparable modifications were reported also when Berkley-HAP nanoparticles were applied (Figure 6B). Frequency of lymphocytes with the late activation marker – CD25, was induced at a substantially lower rate, with an increase observed in the total and CD4+ lymphocytes in the presence of large nHAP (Sigma-HAP). On the contrary, no changes effects were reported in the context of CD8-positive T cells. None of the other selected nano-hydroxyapatites caused any effects on the levels of CD25+ cells in both, CD4 and CD8, and total lymphocytes (Figure 6C).

Hydroxyapatite Nanoparticles' Effects on the Production of Selected Cytokines by Cultured Monocytes and Lymphocytes

The presence of all studied hydroxyapatite nanoparticles led to an increase of TNF-alpha-producing cells in total monocytes at 1000μg/mL, however, in reference to large (Sigma-HAP) and intermediate (Berkley-HAP) nHAP such changes were observed even at a concentration of 500μg/mL. Median changes in TNF-alpha-positive monocytes were least increased in small nHAP (GoHAP Type3) cultures. Noteworthy, only large nHAP caused a prominent increase in the frequency of IL-10+ monocytes starting at 500μg/mL (Figure 7A).

In reference to lymphocyte-related cytokine production, we found that Sigma-HAP at 500μg/mL to 1000μg/mL led to a large increase in the frequency of IFN-gamma+ cells. Interestingly, small nHAP (GoHAP Type1) even caused a slight reduction of IFN-gamma+ lymphocytes at a concentration of 1000μg/mL. As regards IL-10, a transient increase was observed only in samples treated with small nHAP (GoHAP Type1) at 100μg/mL. Elevated level of IL-17A was also observed in the case of 100μg/mL of intermediate nHAP (Berkley-HAP). At higher concentrations, 500 to 1000μg/mL,

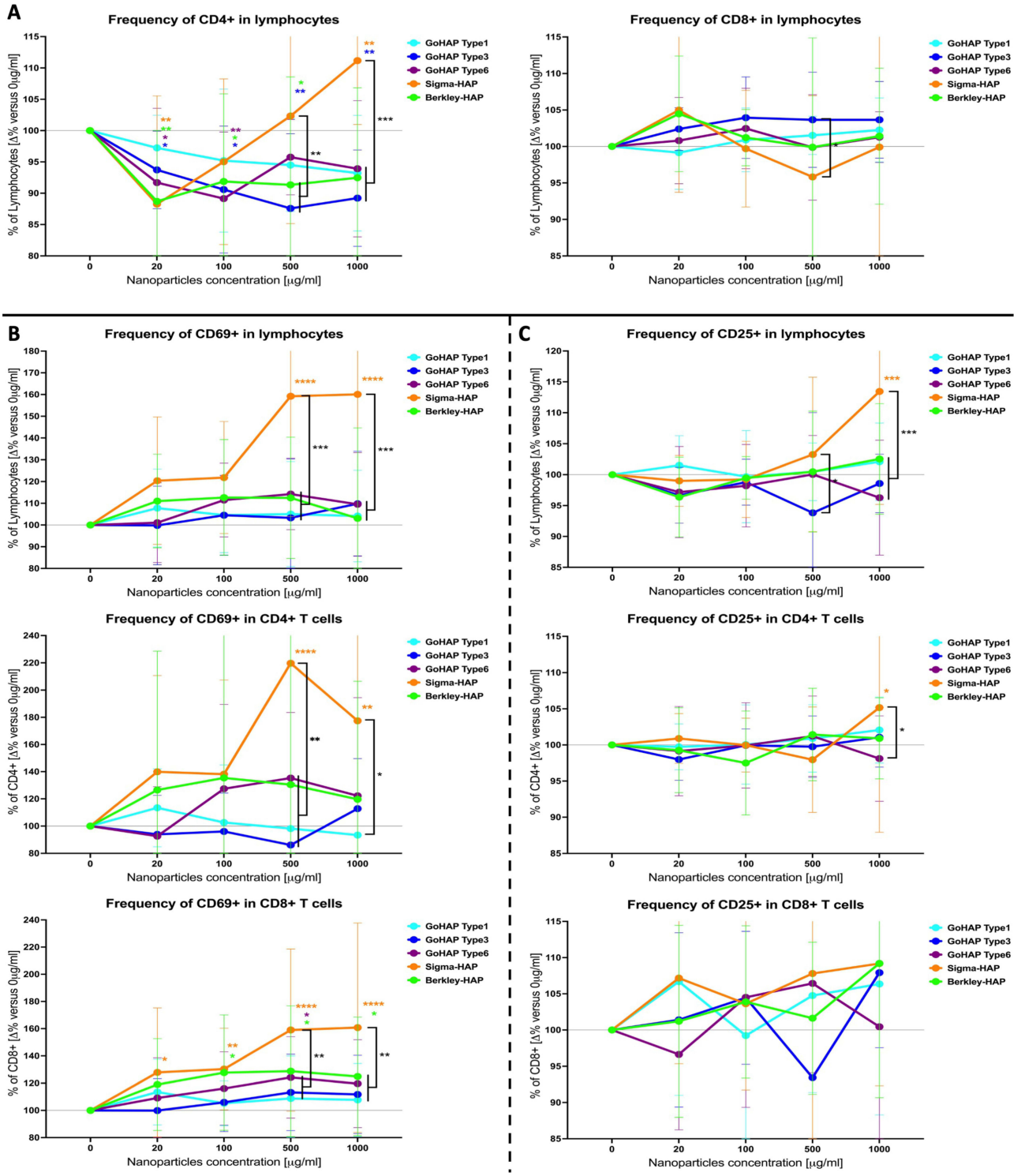

Figure 6 Analysis of frequencies and activation status of lymphocyte subsets stimulated with nano-hydroxyapatites. Changes in CD4+ and CD8+ lymphocytes frequency in presence of nanoparticles (**A**). Assessment of activation markers – CD69 (**B**) and CD25 (**C**), in lymphocyte subsets incubated with hydroxyapatite nanoparticles. Data presented as median change (with interquartile range) versus untreated samples (0μg/mL) (n = 8). Significant differences versus untreated samples were indicated with color asterisks corresponding to selected nanoparticles; brackets demonstrated differences between types of nano-powders at certain concentrations, as determined by two-way ANOVA followed by Fisher's LSD post hoc test. Significance level was set at p value of 0.05: *< 0.05, **< 0.01, ***< 0.001, ****p < 0.0001.

https://doi.org/10.2147/IJN.S555182

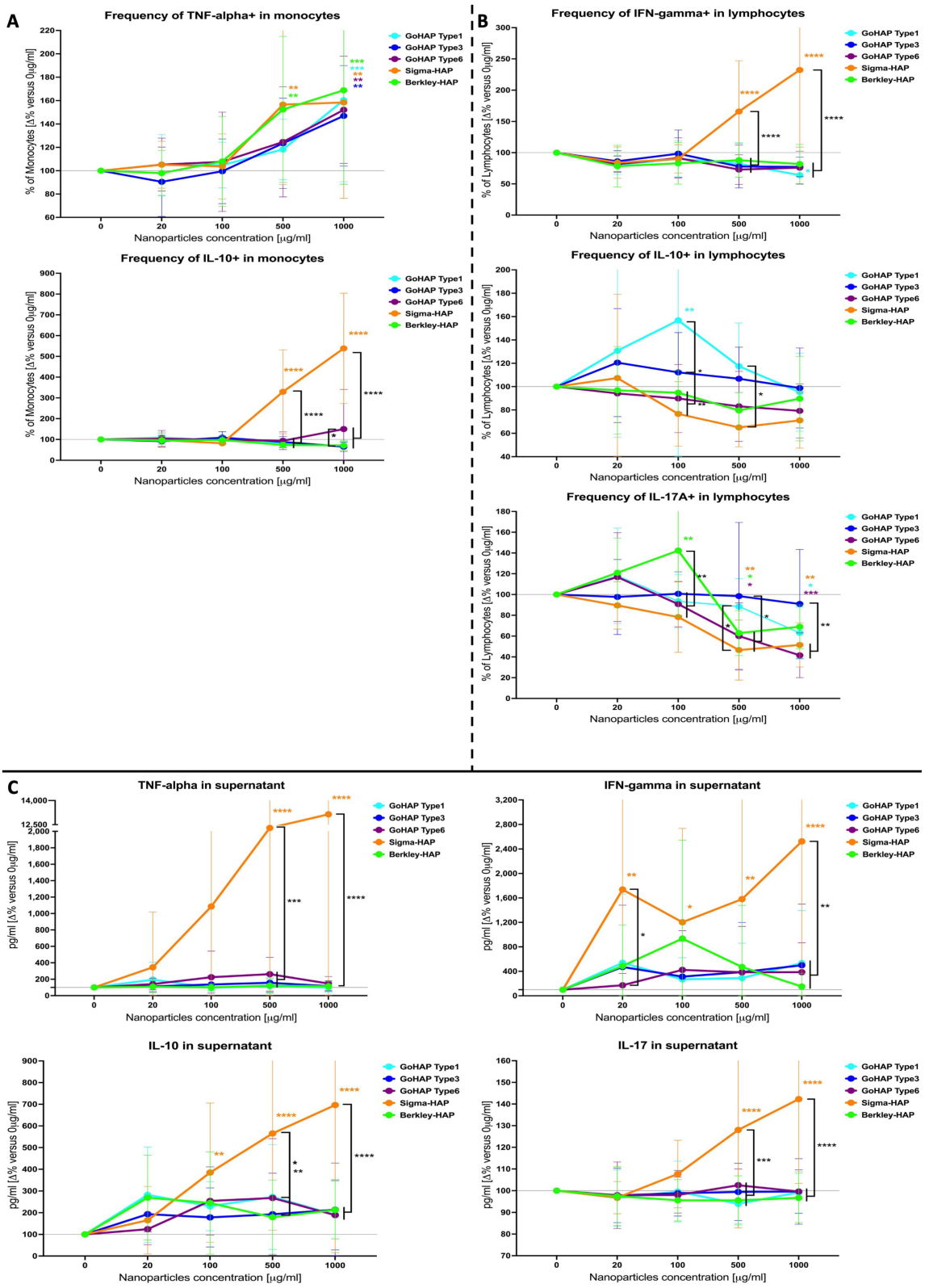

Figure 7 Evaluation of cytokines profile in culture of monocytes and lymphocytes with nanoparticles. Intracellular production of TNF-alpha and IL-10 in monocytes (**A**), and IFN-gamma, IL-10 and IL-17A by lymphocytes in presence of nano-hydroxyapatites (**B**). Assessment of cytokines released by the PBMC incubated with nanoparticles (**C**). Data presented as median change (with interquartile range) versus untreated samples (0μg/mL) (n = 8). Significant differences versus untreated samples indicated with color asterisks corresponding to selected nanoparticles; brackets demonstrated differences between nano-powders at certain concentrations, as determined by two-way ANOVA followed by Fisher's LSD post hoc test. Significance level was set at p value of 0.05: *< 0.05, **< 0.01, ***< 0.001, ****p < 0.0001.

https://doi.org/10.2147/IJN.S555182

IL-17A showed lower values compared to untreated samples, in the presence of two intermediate nHAP (~40-60 nm; GoHAP Type6, Berkley-HAP) and large nHAP (~90-100 nm; Sigma-HAP). Noteworthy, selected small nHAP (~15 nm; GoHAP Type3) seemed to maintain unchanged levels of all tested cytokines among lymphocytes (Figure 7B).

Profiling of the cytokines released by PBMC into culture media confirmed the effects caused by large nHAP (Sigma-HAP). These nanoparticles led to substantial increase in TNF-alpha, especially at 500μg/mL and 1000μg/mL. Similarly, an isolated rise in the presence of large nHAP was observed in reference to IL-17A. A statistically significant influence of that nanohydroxyapatite was shown even at the lowest concentrations in the context of IFN-gamma. A gradual and substantial increase in IL-10 levels was shown with large nHAP (Sigma-HAP) doses of 100μg/mL. Despite slight variations in the presence of other studied nanoparticles, none of them caused significant changes in the analyzed cytokines (Figure 7C).

Influence of Selected Hydroxyapatite Nanoparticles Presence in Culture on Mutual Interactions Between the Tested Subpopulations of Monocytes and Lymphocytes

In general, none of the tested nanoparticles showed substantial disturbance in the mutual association between the tested immune cell subpopulations. Individual changes reported within the selected hydroxyapatite nanoparticles, compared to the untreated samples, were closely related to the significant variations reported above.

Unlike samples without nanoparticles, the application of small nHAP (GoHAP Type1) and intermediate nHAP (GoHAP Type6) resulted in a positive association between TNF-alpha+ and IL-10+ monocytes. At concentration below 1000μg/mL, small nHAP (~8-15 nm; GoHAP Type1 and GoHAP™ Type3) showed diminished association between IFN-gamma+ and IL-10+ (positive) or IL-17A+ (negative) lymphocytes, as reported in untreated cells. In all small to intermediate nHAP of GoHAP-related types of nanoparticles, a positive correlation arose between CD4+ lymphocytes and IL-17A+ subset of those cells. Despite links in untreated PBMCs between monocyte subpopulations and subsets of lymphocytes expressing IFN-gamma, IL-10 or IL-17A, those relations were lost. Some of them were even reversed as shown at higher concentrations of intermediate nHAP (GoHAP Type6), where positive correlations were shown between CD14++CD16+ monocytes and the tested subsets of lymphocytes – IFN-gamma+, IL-10+ and IL-17A+. In reference to large nHAP (Sigma-HAP), correlations between monocyte subsets and both TNF-alpha+ and IL-10+ monocyte subsets, as well as CD4+ lymphocytes were observed. The same nanoparticles diminished or reversed the association between IL-17A+ and IFN-gamma+ or IL-10+ lymphocytes. The same phenomenon was observed in the context of monocyte subpopulations' link to the selected cytokine-expressing lymphocyte subsets reported in PBMC samples with no presence of nanoparticles. Nanohydroxyapatites of intermediate size (~51 nm; Berkley-HAP) showed a similarity to the effects caused by large nHAP (Sigma-HAP) in the term of correlation between monocyte subsets and TNF-alpha+ or IL-10+ producing monocytes. In contrast, especially at concentrations of below 1000μg/mL, incubation with intermediate nHAP (Berkley-HAP) preserved the associations between monocyte subpopulations and the same lymphocyte subsets observed in untreated samples (Figure 8).

Discussion

Nanomaterials due to their invaluable properties find their application in nearly all aspects of life. Despite significant advancement in the field, nanoparticles influence on our organism is predominantly limited to studies on general biocompatibility of the selected material and exclusion of cytotoxic effects.[5,27,28] However, data on how these materials affect our immune system are scarce and require clarification due to potentially critical impact on our health. To date there were no studies revealing direct nano-hydroxyapatite (nHAP) influence on healthy human immune cells. This comes as quite a surprise considering their vast clinical application potential for example in various types of cancer currently being widely investigated.[29,30] Here, for the first time we provided an in-depth evaluation of hydroxyapatite nanoparticles' different sizes effects on immunity-related cellular and humoral aspects.

Considering the effects of nano-hydroxyapatites in reference to cell viability, Zhang et al reported using VX2 rabbit carcinoma cell line's proapoptotic effect of nano-sized hydroxyapatites. Decrease in cell viability was found to start at a concentration of 100μg/mL and demonstrated a dose- and time-dependent manner.[28] Interestingly, intermediate to large

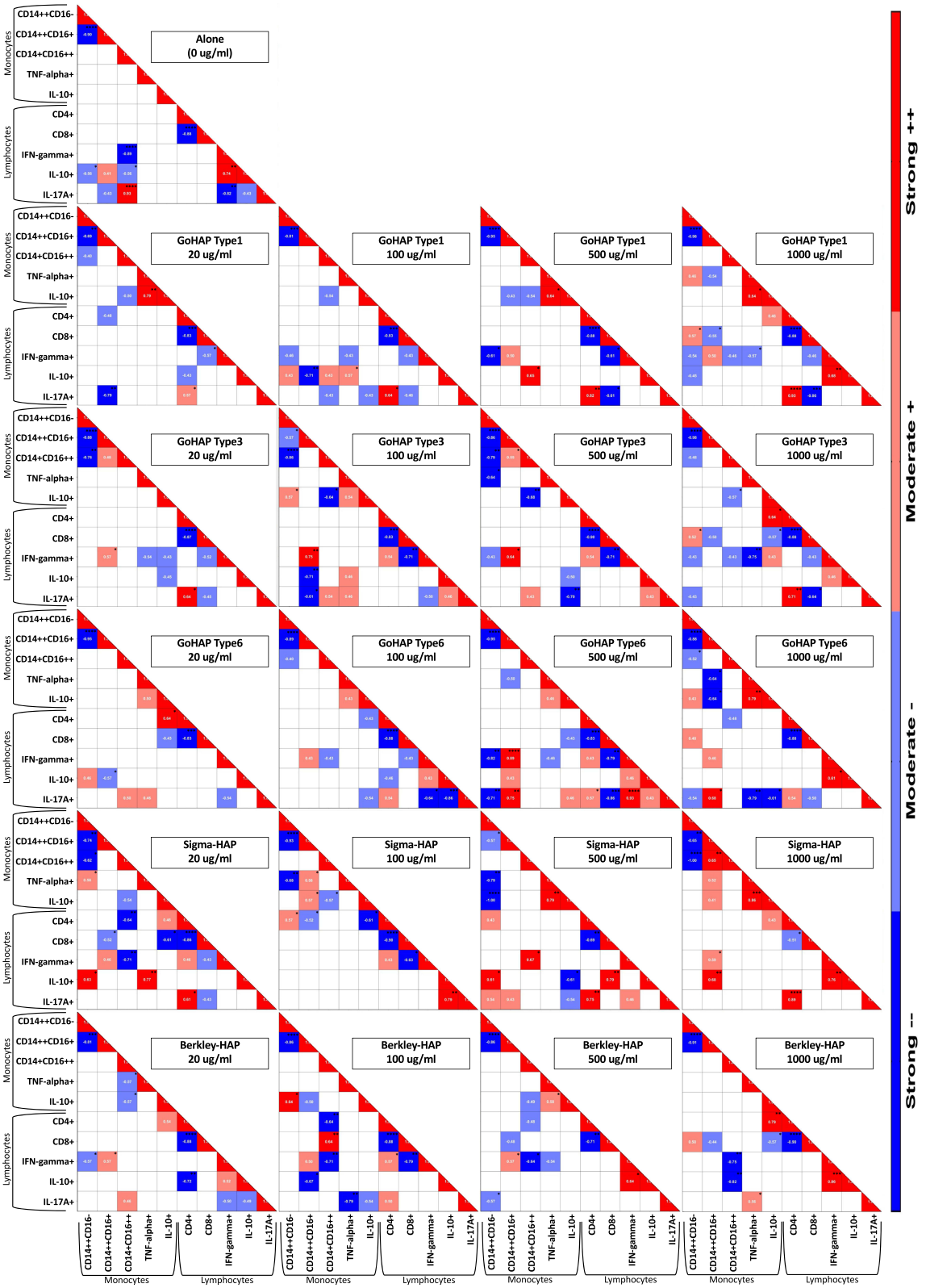

Figure 8 Mutual correlations of analyzed immune cell populations in presence of selected hydroxyapatite nanoparticles. Data presented as individual heatmap for each type and concentration of nanoparticle; with correlation coefficient r value, as determined Spearman correlation test, presented and highlighted with color (blue and red corresponding to negative and positive values respectively). Only correlations of moderate (-/+0.40 to -/+0.59) and strong (-/+0.60 to -/+1.00) associations are shown. Significance level was set at p value of 0.05 and indicated on the graph with asterisks: *< 0.05, **< 0.01, ***< 0.001, ****p < 0.0001.

https://doi.org/10.2147/IJN.S555182

nHAP (~96 nm, Sigma-HAP; (~51 nm, Berkley-HAP) caused the most significant variations in viability of peripheral blood immune cells – monocytes and lymphocytes. Noteworthy, disturbances in live cells frequency were predominantly observed at a concentration of 500μg/mL and higher. Moreover, our data indicate that size of particles might have a significant influence on hydroxyapatite properties even at the nano-scale range, as reported changes were usually observed at size larger than 40nm, starting with intermediate nHAP (~40-60 nm; GoHAPType6 and Berkley-HAP) and through large nHAP (~90-100 nm; Sigma-HAP). That is partially in consent with the study on nano-sized hydroxyapatite influence on osteosarcoma, where the highest aspect ratio of the particles was associated with the most favorable effects obtained.[30] A significant induction of apoptosis was observed with nano-hydroxyapatites of average sizes of 184nm or larger.[31] Flow cytometric analyses were supported by LDH activity in culture supernatants, with deleterious effects observed at the highest concentrations of large nHAP (Sigma-HAP). That is in contrast with data on VX2 carcinoma cells where hydroxyapatites at micro level in size seemed to exert less pronounced apoptotic effects.[28] Most stable conditions, with no changes in viability-related parameters, were obtained in the presence of small nHAP (~15 nm; GoHAP Type3) nano-hydroxyapatites. Similar lack of viability reduction was observed in dendritic cells stimulated by rod-shaped hydroxyapatites at similar nano-level size.[32] Additionally, no disturbances in viability were reported when treating macrophages in vitro with nano-hydroxyapatites with mean size between 60nm and 70nm, when in vitro treating macrophages.[33]

In accordance, the use of nano-hydroxyapatites should be preceded by the assessment of their effects on specific tissues as certain types and concentrations can affect not only cancerous but also healthy cells. In the study involving mice breast cancer cell line 4T1, the effectively cytotoxic concentration was the maximal concentration used in the current study (1000μg/mL). Thus, aside from the expected anti-cancer effects, serious adverse reactions can be observed within healthy cells.[27,34] On the other hand, study on nanocomposite hydrogels with hydroxyapatite supported the survival of stem cells and osteogenesis.[4] Various responses to nano-hydroxyapatites were reported in in vitro models of healthy and cancer cells. Squamous cell cancer line (VX2 cell line) viability was reduced at the nanoparticles concentration starting at 250μg/mL. Interestingly, no deleterious effects at doses below 1000μg/mL were reported in healthy mice fibroblasts (L929 cell line).[28] Despite slight differences observed, mostly as a result of two different models - cancer and healthy immune cells, those results shed a new light on proper selection of nano-hydroxyapatites without unfavorable cytotoxic effects on immune cells.

Among all tested nanoparticles, large nHAP (Sigma-HAP) caused the highest changes in the internal structure of monocytes, most possibly resulting from phagocytosis of those relatively large particles. The possibility of nano-hydroxyapatite internalization was previously suggested in reference to the epithelial-like cells of the CHO cell line.[27] Here, changes in granularity were also followed by a slight increase in the cell size. Interestingly, a similar direction of elevated granularity was observed in response to intermediate nHAP (GoHAP Type6). Those nanoparticles showed close similarity to large nHAP (like Sigma-HAP) parameters obtained in thermogravimetric analysis. The remaining types of nano-hydroxyapatites did not cause a substantial impact on the morphology of the monocytes in the course of their phagocytic activity. In another study nanoparticles with larger sizes (from 150nm to 400nm) were also found to cause changes in macrophage granularity as shown here. Those size-dependent variations were also confirmed with microscopic visualization of the engulfed fluorescein-stained hydroxyapatites.[35] Observed variations cannot be simply explained by nanoparticle size as both intermediate nHAP - GoHAP Type6 and Berkley-HAP, demonstrated relatively similar mean particle size (40μm and 51μm respectively; SMD_{BET}). Close similarities we found to be potentially associated with comparable thermogravimetric characteristics of both nano-hydroxyapatites. In addition, in contrast to Berkley-HAP, GoHAP Type6 had higher values of total pore volume (TPV). Interestingly, large nHAP (Sigma-HAP), at concentration between 500μg/mL and 1000μg/mL, exclusively induced changes in all three monocyte subsets. We reported an increase in the dominant peripheral subset – classical monocytes (CD14++CD160-), and "pro-inflammatory" non-classical monocytes (CD14+CD16++). On the contrary, another subset of CD16-positive monocytes, namely intermediate monocytes (CD14++CD16+), showed reduced frequency at high levels of those nanoparticles. A less intense decline was additionally observed in the presence of intermediate nHAP (GoHAP Type6). Reported changes in monocytes, together with a previously revealed increase in genes related to M1 macrophages when in the presence nano-hydroxyapatite,[28] might indicate selective differentiation of monocytes towards more pro-inflammatory subsets. That is

furthermore supported by another study demonstrating polarization of macrophage phenotype towards M1 subset (dominance of CD86 and F4/80 versus CD80 and CD206 surface markers) in the presence of these nanoparticles.[30,33] Thus, commercial Sigma-HAP nanoparticles application was associated with an unfavorable disturbance in the balance between inflammatory and anti-inflammatory populations (IL-10-producing intermediate monocytes). Most recent studies indicated a substantial reduction of monocytes and macrophages within the tumor environment in the presence of hydroxyapatite, suggesting suppressing effects of these nanoparticles.[29] Noteworthy, hydroxyapatite surfaces were shown to induce proliferation of osteoblast- and macrophage-like cells in homogenous cell cultures, with no presence of cancer cells.[36] Present macrophages can be simultaneously polarized towards a tumoricidal phenotype, especially when combined with immunomodulatory TLR (Toll-like receptors) agonists.[34] Additionally, we showed that such phenomenon might strictly be associated with the type of the nano-hydroxyapatite used, including differences in size, specific surface area or thermogravimetric properties. Here, only large nHAP (Sigma-HAP) caused beneficial, in the context of the cancerous process, reduction of immunosuppressive subset in favor of pro-inflammatory monocytes.

Influence of the large nHAP (Sigma-HAP) was not only limited to the phenotypic changes within monocytes. We found that the nanoparticles use led to an excessive activation of all tested monocyte subpopulations, demonstrating the most substantial changes in CD16-positive cells. That was confirmed with an increase in the level of CD69+ monocytes, which is an early activation marker with induced presence on the surface of monocytes.[37,38] In consent with our data, previous research on mice macrophages revealed a promotion of the innate immunities Toll-like receptor (TLR9) and enhanced response to stimulation with CpG (present in microbial genomes) when nano-hydroxyapatites were applied.[39] Assessment of CD163 on the surface of monocytes allowed us to complete the previous observation of monocytes shift towards non-classical monocytes with concomitant decline in the intermediate subsets. That results from the fact that CD163 is closely related to the alternative activation of the monocytes and their differentiation into M2 macrophages, predominantly from the subset of intermediate monocytes.[40–42] Here, we found significant reduction of all the monocyte subpopulations expressing CD163 in the presence of large tested nanoparticles. Slight drop in frequency was also reported in the presence of intermediate (GoHAP Type6) and small (GoHAP Type1) nHAP, affecting CD163-positive non-classical monocytes. Recently, it has been shown that the composition of the nanoparticles can significantly affect biomaterials influence on macrophages. Tricalcium phosphate hydroxyapatite showed higher induction of inflammatory response through macrophage-derived release of extracellular traps (METs). In contrast, those materials with reduced content of calcium were not only deprived of the above-mentioned effects, but also promoted polarization of macrophages toward the M2 phenotype.[43] Interestingly, within inflammatory conditions hydroxyapatite nanoparticles surfaces were shown to induce alternative activation of macrophages, with an increase in CD163, CD203 and Arg-1.[44] As 100–150nm nano-hydroxyapatites induced the M2 phenotype,[45] further experiments might be needed to establish whether the reported here reduced frequency of intermediate monocytes is associated with their differentiation into immunosuppressive macrophages. In accordance with the data above, here for the first time, we showed the beneficial effects of novel hydroxyapatite nanoparticles on monocytes development. Lack of disturbances in phagocytes morphology together with preserving proper distribution of the peripheral blood monocytes, support high biocompatibility with no signs of immunogenicity, in the context of innate immunity cells. Noteworthy, the process of production is crucial as in the current study most beneficial effects were observed when small nHAP (GoHAP Type3) was implemented. Therefore, their application in human-related products or medical setting seems to be associated with no risk of both, inflammatory reactions or unfavorable immunosuppression.

Contrary to monocytes, the tested nanoparticles did not cause such substantial changes in the frequency of CD4+ (helper) T or CD8+ (cytotoxic) T lymphocytes. First, no changes, at any concentration, were reported in reference to CD8 + T cells. All nano-hydroxyapatites initially reduced the frequency of CD4+ lymphocytes with a slight decline maintained up to the highest concentration tested. However, the presence of large nHAP (Sigma-HAP) led to a gradual increase from 20μg/mL resulting in the significantly elevated level of helper T cells at 1000μg/mL. Micro-sized hydroxyapatites were the only ones (compared to nanoparticles) increasing the numbers of CD3+ lymphocytes within the femoral bone defect.[45] In contrast, a mice model of osteosarcoma revealed an increase of CD8+ T cells population in the presence of nano-hydroxyapatites, at the highest rate within the tumor site compared to the spleen, but predominantly using specific needle-shaped particles.[30] Moreover, nanoparticles of large size were not neutral in the context of

lymphocyte activation, with an elevated early activation marker (CD69) demonstrated at concentrations starting at 500μg/mL. Another intermediate size nano-hydroxyapatite (Berkley-HAP), also caused an elevation of CD69+ within the population of cytotoxic CD8+ lymphocytes. In accordance, nano-hydroxyapatites with size of 50nm and larger were shown previously to induce higher expression of genes related to the activity of natural killer (NK) cells, anti-tumor mediators and leukocyte migration within the cancer niche.[28] Lymphocytes expressing late activation CD25+ marker were the only affected by the highest dosage of Sigma-HAP nanoparticles, with no changes found in the status of late activated CD4+ cells. In the previous study, significantly higher values of size and surface ratio within nano-hydroxyapatites were associated with a profound impact on the activation and migration of CD8+ lymphocytes, as adjuvants required for stimulation with the viral antigen.[35] Similarly, hydroxyapatite spheres loaded with strontium substantially improved the response of CD4+ and CD8+ T cells to stimulation with a specific allergen.[8] Lymphocyte-related changes reported here revealed substantial influence of the size and hydroxyapatite type. Subsequent studies might demonstrate the role of those variations in the course of selected conditions, including autoimmune, inflammatory and cancer diseases. That would allow for the establishment of novel potential clinical applications of the hydroxyapatite nanoparticles.

Cytokine production by peripheral blood cells was predominantly affected by large nHAP (Sigma-HAP), especially within the range of 20μg/mL to 500μg/mL. Apart from inducing an increase in pro-inflammatory cytokines, higher values of IL-10 were observed – clearly associated with the production within monocytes. Other tested nanoparticles did not exert significant changes in the cytokines released into the medium. In contrast, all types used elevated TNF-alpha within monocytes, with concomitant decline in IL-17A in lymphocytes. Interestingly, other source of IL-17A was activated due to general increase in that cytokine in supernatants in the presence of high Sigma-HAP doses. It seems that only particles with a diameter of around 100nm caused the most substantial disturbances in pro- and anti-inflammatory cytokine balance. Similarly, an increase in TNF-alpha, together with MCP-1, was reported previously at the mRNA and protein level.[28,46] Macrophages, as the last stage of monocyte differentiation, were also shown to release higher amounts of TNF-alpha in the presence of hydroxyapatites exceeding 50nm in size, with concomitant rise in MCP-1.[28,33,34] Effects of nano-hydroxyapatites' size and aspect ratio effects on the inflammatory response were also reported recently. In a corresponding study only particles larger than 100–150nm caused a significant increase in IL-1beta - another pro-inflammatory cytokine.[35] That was also confirmed on the macrophages in vitro with elevated TNF-alpha, IL-1beta and IL-1alpha in the presence of large nano-hydroxyapatites (1μm to 1.5μm), at the concentration of 250μg/mL.[45] Here, we demonstrated for the first time that the use of large-sized nanoparticles of hydroxyapatite can additionally cause an increase in anti-inflammatory IL-10 release, presumably associated with monocytes predominantly. That is in contrast with presented previously reduced IL-10 production by mice macrophages in the presence of high (1000μg/mL) concentration of nano-hydroxyapatites.[39] In addition, macrophage-based experiments revealed higher levels of IL-10 when the nanoparticles of around 100–150nm were administered, compared to large-sized hydroxyapatites.[45] However, we presume that the changes reported here might be related to the presence of other immune cells in the microenvironment and mechanisms controlling the balance between pro- and anti-inflammatory factors. In fact, in a diabetic in vivo rat model the pro-inflammatory environment was modulated by nano-hydroxyapatites presence leading to higher expression of another immunosuppressive cytokine – TGF-beta.[44] A concomitant increase in immunosuppressive cytokines, apart from elevated TNF-alpha, was suggested as a limitation of potential nano-hydroxyapatite application in the induction of anti-tumor responses.[30]

Functional response of acquired immunity cells to nano-hydroxyapatites was associated with an increase in IFN-gamma production by lymphocytes. Interestingly, changes were observed after large 100nm hydroxyapatites application starting at 500μg/mL thus explaining no effects observed in previous studies using dendritic cells, where lower concentrations were tested.[32] More efficient induction of IFN-gamma release by lymphocytes, cytotoxic CD8+ specifically, was reported when nanoparticles exceeding 300nm were applied to stimulation with viral antigen (HbsAg).[35] Higher values of IFN-gamma were also reported at the site of bone injury in mice, treated with implant consisting hydroxyapatites larger that 1μm.[45] Excluding the limited increase of TNF-alpha within monocytes at the highest dose, small-sized GoHAP nano-hydroxyapatites demonstrated the highest biocompatibility and no induction of inflammation.

Considering numerous potential applications, selection of proper nano-hydroxyapatite should be considered in the context of its immunogenicity. On one hand, certain forms can be beneficial in the context of additional induction of immune responses at the site of ongoing neoplastic process or even direct killing and inhibition of cancer cells.[29–31] On

the other hand, some of the small-sized hydroxyapatite nanoparticles, like presented here, might allow for complete avoidance of the immune system reactivity providing the highest rate of biocompatibility – crucial in the treatment of injuries and transplantology. At the same time, in the context of bone-related applications, we must select nano-hydroxyapatites with eventual additives allowing higher osteogenic potential than currently available materials.[3,28,44,45] Data presented here clearly demonstrated the immunomodulatory potential of nano-hydroxyapatites in a structural- and dose-dependent manner. Further research in this field is of great importance to distinguish the most suitable applications for the tested nanoparticles. Not only in the development of the most biocompatible and non-immunogenic materials for implants, but also in therapeutic approaches aimed at the immune system directly or supporting responses in anti-cancer procedures.

Conclusions

Nanoparticles, particularly nano-hydroxyapatite (nHAP), are extensively used due to their unique properties, but their effects on the immune system are not well studied to date, justifying the need for research in that field. Here, we showed that commercial nHAPs like Sigma and Berkley significantly affect immune cell viability, with particle size influencing those changes. On the other hand, small nHAP (GoHAP Type3) showed no adverse effects on cell viability. Changes in the monocyte morphology indicated a phagocytic process of the tested nanoparticles, influenced by size and thermogravimetric properties. Shift towards inflammatory activity was reported with an increase in non-classical and a decline of intermediate monocytes. Large nHAP (Sigma-HAP) was found to induce higher levels of CD4+ T cells and activation of lymphocytes. The same nHAP led to the most notable changes in cytokines increasing both, pro- and anti-inflammatory proteins. In addition, all nHAPs raised TNF-alpha levels in monocytes and reduced IL-17A in lymphocytes, with the highest influence of large-sized nanoparticles. No substantial differences between nHAPs types were reported in reference to mutual immune cells correlations. Slight variations of those interactions were affected by increasing doses of high-sized nanoparticles.

Proper nHAP selection is crucial for balancing immune status and biocompatibility, thus its efficient use in clinical applications, including traumas and transplantology. Small-sized nHAPs may reduce the risk of immune reactivity, whereas certain nHAPs could aid in cancer treatment by enhancing immune responses or directly inhibiting cancer cells. Those hypotheses, however, require further research in specific fields.

Taken together, the results of this study support the concept that nanoparticle size represents a dominant parameter governing the immunological behavior of nano-hydroxyapatites, with small-sized particles exhibiting high biocompatibility and larger-sized particles exerting pronounced immunomodulatory effects. While the present work focused on representative nanoparticle formulations spanning distinct size ranges, it does not allow for a continuous or threshold-based analysis across narrowly defined nanoparticle diameters. Future studies employing systematically graded nanoparticle sizes, combined with controlled surface and structural parameters, will be essential to further refine size-dependent immune response profiles and to identify optimal nanoparticle characteristics for specific clinical applications.

Data Sharing Statement

All presented data and corresponding protocols are available upon request from the corresponding author of the paper.

Ethics Approval and Consent to Participate

The informed consent was obtained from all the subjects enrolled in the study. The study was conducted in accordance with the Declaration of Helsinki, and the Local Bioethical Committee in Bialystok approved the implemented study protocol, approval number: APK.002.272.2020.

Consent for Publication

All the authors approved the final version of the manuscript and its publication.

Author Contributions

All authors made a significant contribution to the work reported, whether that is in the conception, study design, execution, acquisition of data, analysis and interpretation, or in all these areas; took part in drafting, revising or critically

reviewing the article; gave final approval of the version to be published; have agreed on the journal to which the article has been submitted; and agree to be accountable for all aspects of the work.

Funding

This research was financially supported by the National Centre for Research and Development within the project "Method of treatment of large bone defects in oncological patients using in vivo tissue engineering approach" (STRATEGMED3/306888/3/NCBR/2017). A part of the research study was conducted on equipment funded by the project Center for Preclinical Research and Technology - CePT II (RPMA.01.01.00-14-8476/17-04) from Regional Operational Programme of the Mazowieckie Voivodeship 2014–2020. A part of the research study was funded by Polish National Centre for Research and Development (NCBR) project NANOLIGABOND (POIR.04.01.02-00-0016/16); 2016-2019.

Disclosure

Professor Marcin Moniuszko reports personal fees, non-financial support from Industry-supported lectures and conferences, outside the submitted work. All authors declare no conflicts of interest.

References

1. Trzaskowska M, Vivcharenko V, Benko A, et al. Biocompatible nanocomposite hydroxyapatite-based granules with increased specific surface area and bioresorbability for bone regenerative medicine applications. *Sci Rep*. 2024;14(1):28137. doi:10.1038/s41598-024-79822-0
2. Han Y, Li S, Cao X, et al. Different inhibitory effect and mechanism of hydroxyapatite nanoparticles on normal cells and cancer cells in vitro and in vivo. *Sci Rep*. 2014;4(1):7134. doi:10.1038/srep07134
3. Sultan N, Jayash SN. Evaluation of osteogenic potential of demineralized dentin matrix hydrogel for bone formation. *BMC Oral Health*. 2023;23 (1):247. doi:10.1186/s12903-023-02928-w
4. Fu M, Li J, Liu M, et al. Sericin/Nano-hydroxyapatite hydrogels based on graphene oxide for effective bone regeneration via immunomodulation and osteoinduction. *Int J Nanomed*. 2023;18:1875–1895. doi:10.2147/IJN.S399487
5. Abedi F, Moghaddam SV, Ghandforoushan P, et al. Synthesis and characterization of growth factor free nanoengineered bioactive scaffolds for bone tissue engineering. *J Biol Eng*. 2022;16(1):28. doi:10.1186/s13036-022-00303-x
6. Do TN, Lee W-H, Loo C-Y, et al. Hydroxyapatite nanoparticles as vectors for gene delivery. *Ther Deliv*. 2012;3(5):623–632. doi:10.4155/tde.12.39
7. Huggins RJ, Mendelson BC. Biologic behavior of hydroxyapatite used in facial augmentation. *Aesthetic Plast Surg*. 2017;41(1):179–184. doi:10.1007/s00266-016-0707-9
8. Garbani M, Xia W, Rhyner C, et al. Allergen-loaded strontium-doped hydroxyapatite spheres improve allergen-specific immunotherapy in mice. *Allergy*. 2017;72(4):570–578. doi:10.1111/all.13041
9. Adamiano A, Iafisco M, Sandri M, et al. On the use of superparamagnetic hydroxyapatite nanoparticles as an agent for magnetic and nuclear in vivo imaging. *Acta Biomater*. 2018;73:458–469. doi:10.1016/j.actbio.2018.04.040
10. Badea ML, Iconaru SL, Groza A, et al. Peppermint essential oil-doped hydroxyapatite nanoparticles with antimicrobial properties. *Molecules*. 2019;24(11):2169. doi:10.3390/molecules24112169
11. Lange T, Schilling AF, Peters F, et al. Proinflammatory and osteoclastogenic effects of beta-tricalciumphosphate and hydroxyapatite particles on human mononuclear cells in vitro. *Biomaterials*. 2009;30(29):5312–5318. doi:10.1016/j.biomaterials.2009.06.023
12. Guo M, Dong Y, Xiao J, et al. In vivo immuno-reactivity analysis of the porous three-dimensional chitosan/SiO2 and chitosan/SiO2/hydroxyapatite hybrids. *J Biomed Mater Res A*. 2018;106(5):1223–1235. doi:10.1002/jbm.a.36320
13. Motskin M, Wright DM, Muller K, et al. Hydroxyapatite nano and microparticles: correlation of particle properties with cytotoxicity and biostability. *Biomaterials*. 2009;30(19):3307–3317. doi:10.1016/j.biomaterials.2009.02.044
14. Huang J, Best SM, Bonfield W, et al. In vitro assessment of the biological response to nano-sized hydroxyapatite. *J Mater Sci Mater Med*. 2004;15 (4):441–445. doi:10.1023/B:JMSM.0000021117.67205.cf
15. Turkez H, Yousef MI, Sönmez E, et al. Evaluation of cytotoxic, oxidative stress and genotoxic responses of hydroxyapatite nanoparticles on human blood cells. *J Appl Toxicol*. 2014;34(4):373–379. doi:10.1002/jat.2958
16. Matesanz MC, Feito MJ, Oñaderra M, et al. Early in vitro response of macrophages and T lymphocytes to nanocrystalline hydroxyapatites. *J Colloid Interface Sci*. 2014;416:59–66. doi:10.1016/j.jcis.2013.10.045
17. Rydén L, Omar O, Johansson A, et al. Inflammatory cell response to ultra-thin amorphous and crystalline hydroxyapatite surfaces. *J Mater Sci Mater Med*. 2017;28(1):9. doi:10.1007/s10856-016-5814-2
18. Velard F, Schlaubitz S, Fricain J-C, et al. In vitro and in vivo evaluation of the inflammatory potential of various nanoporous hydroxyapatite biomaterials. *Nanomedicine*. 2015;10(5):785–802. doi:10.2217/nnm.15.12
19. Liu X, Sun J. Potential proinflammatory effects of hydroxyapatite nanoparticles on endothelial cells in a monocyte-endothelial cell coculture model. *Int J Nanomed*. 2014;9:1261–1273. doi:10.2147/IJN.S56298
20. Santavirta S, Nordstrm D, Ylinen P, et al. Biocompatibility of hydroxyapatite-coated hip prostheses. *Arch Orthop Trauma Surg*. 1991;110(6):288–292. doi:10.1007/BF00443460
21. Smolen D. Method for producing synthetic hydroxyapatite nanoplates and nanopowder containing synthetic hydroxyapatite nanoplate. Poland: Institute of High Pressure Physics; 2014.

22. Kuśnieruk S, Wojnarowicz J, Chodara A, et al. Influence of hydrothermal synthesis parameters on the properties of hydroxyapatite nanoparticles. *Beilstein J Nanotechnol*. 2016;7:1586–1601. doi:10.3762/bjnano.7.153
23. Szałaj U, Świderska-środa A, Chodara A, et al. Nanoparticle size effect on water vapour adsorption by hydroxyapatite. *Nanomaterials*. 2019;9 (7):1005. doi:10.3390/nano9071005
24. Rogowska-Tylman J, Locs J, Salma I, et al. In vivo and in vitro study of a novel nanohydroxyapatite sonocoated scaffolds for enhanced bone regeneration. *Mater Sci Eng C Mater Biol Appl*. 2019;99:669–684. doi:10.1016/j.msec.2019.01.084
25. Pielaszek R. Analytical expression for diffraction line profile for polydispersive powders. In: *XIX Conference on Applied Crystallography*. Krakow; 2004. p. 43–50.
26. Pielaszek R. FW15/45M method for determination of the grain size distribution from powder diffraction line profile. *J Alloy Compd*. 2004;382 (37):128–132. doi:10.1016/j.jallcom.2004.05.040
27. Oberbek P, Bolek T, Chlanda A, et al. Characterization and influence of hydroxyapatite nanopowders on living cells. *Beilstein J Nanotechnol*. 2018;9:3079–3094. doi:10.3762/bjnano.9.286
28. Zhang K, Zhou Y, Xiao C, et al. Application of hydroxyapatite nanoparticles in tumor-associated bone segmental defect. *Sci Adv*. 2019;5(8): eaax6946. doi:10.1126/sciadv.aax6946
29. Chen S, Xing Z, Geng M, et al. Macrophage fusion event as one prerequisite for inorganic nanoparticle-induced antitumor response. *Sci Adv*. 2023;9(29):eadd9871. doi:10.1126/sciadv.add9871
30. Wu H, Wang R, Li S, et al. Aspect ratio-dependent dual-regulation of the tumor immune microenvironment against osteosarcoma by hydroxyapatite nanoparticles. *Acta Biomater*. 2023;170:427–441. doi:10.1016/j.actbio.2023.08.046
31. Cui X, Liang T, Liu C, et al. Correlation of particle properties with cytotoxicity and cellular uptake of hydroxyapatite nanoparticles in human gastric cancer cells. *Mater Sci Eng C Mater Biol Appl*. 2016;67:453–460. doi:10.1016/j.msec.2016.05.034
32. Wang X, Li X, Ito A, et al. Rod-shaped and substituted hydroxyapatite nanoparticles stimulating type 1 and 2 cytokine secretion. *Colloids Surf B Biointerfaces*. 2016;139:10–16. doi:10.1016/j.colsurfb.2015.12.004
33. Hua Y, Wu J, Wu H, et al. Exposure to hydroxyapatite nanoparticles enhances Toll-like receptor 4 signal transduction and overcomes endotoxin tolerance in vitro and in vivo. *Acta Biomater*. 2021;135:650–662. doi:10.1016/j.actbio.2021.09.006
34. Wang R, Hua Y, Wu H, et al. Hydroxyapatite nanoparticles promote TLR4 agonist-mediated anti-tumor immunity through synergically enhanced macrophage polarization. *Acta Biomater*. 2023;164:626–640. doi:10.1016/j.actbio.2023.04.027
35. Zhang L, Liang Z, Chen C, et al. Engineered hydroxyapatite nanoadjuvants with controlled shape and aspect ratios reveal their immunomodulatory potentials. *ACS Appl Mater Interf*. 2021;13(50):59662–59672. doi:10.1021/acsami.1c17804
36. Dabbah K, Perelshtein I, Gedanken A, et al. Effects of a ZnCuO-nanocoated Ti-6Al-4V surface on bacterial and host cells. *Materials*. 2022;15 (7):2514. doi:10.3390/ma15072514
37. Wöbke TK, von Knethen A, Steinhilber D, et al. CD69 is a TGF-β/1α,25-dihydroxyvitamin D3 target gene in monocytes. *PLoS One*. 2013;8(5): e64635. doi:10.1371/journal.pone.0064635
38. De Maria R, Cifone MG, Trotta R, et al. Triggering of human monocyte activation through CD69, a member of the natural killer cell gene complex family of signal transducing receptors. *J Exp Med*. 1994;180(5):1999–2004. doi:10.1084/jem.180.5.1999
39. Zeng Q, Wang R, Hua Y, et al. Hydroxyapatite nanoparticles drive the potency of Toll-like receptor 9 agonist for amplified innate and adaptive immune response. *Nano Res*. 2022;15(10):9286–9297. doi:10.1007/s12274-022-4683-x
40. Moestrup SK, Møller HJ. CD163: a regulated hemoglobin scavenger receptor with a role in the anti-inflammatory response. *Ann Med*. 2004;36 (5):347–354. doi:10.1080/07853890410033171
41. Yang J, Zhang L, Yu C, et al. Monocyte and macrophage differentiation: circulation inflammatory monocyte as biomarker for inflammatory diseases. *Biomark Res*. 2014;2(1):1. doi:10.1186/2050-7771-2-1
42. Italiani P, Boraschi D. From monocytes to M1/M2 macrophages: phenotypical vs functional differentiation. *Front Immunol*. 2014;5:514. doi:10.3389/fimmu.2014.00514
43. Seifert A, Tylek T, Blum C, et al. Calcium phosphate-based biomaterials trigger human macrophages to release extracellular traps. *Biomaterials*. 2022;285:121521. doi:10.1016/j.biomaterials.2022.121521
44. Li Y, Yang L, Hou Y, et al. Polydopamine-mediated graphene oxide and nanohydroxyapatite-incorporated conductive scaffold with an immunomodulatory ability accelerates periodontal bone regeneration in diabetes. *Bioact Mater*. 2022;18:213–227. doi:10.1016/j.bioactmat.2022.03.021
45. Mahon OR, Browe DC, Gonzalez-Fernandez T, et al. Nano-particle mediated M2 macrophage polarization enhances bone formation and MSC osteogenesis in an IL-10 dependent manner. *Biomaterials*. 2020;239:119833. doi:10.1016/j.biomaterials.2020.119833
46. Ding T, Sun J. Mechanistic understanding of cell recognition and immune reaction via CR1/CR3 by HAP- and SiO2 -NPs. *Biomed Res Int*. 2020;2020(1):7474807. doi:10.1155/2020/7474807